Voltage-gated sodium channel blockers as cytostatic inhibitors of the androgen-independent prostate cancer cell line PC-3

James D. Anderson,[1] Todd P. Hansen,[1] Paul W. Lenkowski,[1] Alison M. Walls,[3] Indrani M. Choudhury,[1] Hilary A. Schenck,[1] Mati Friehling,[1] Genevieve M. Höll,[1] Manoj K. Patel,[2] Robert A. Sikes,[3] and Milton L. Brown[1]

[1]Departments of Chemistry and [2]Anesthesiology, University of Virginia, Charlottesville, VA, and [3]Department of Biological Sciences, University of Delaware, Newark, DE

Abstract

The recent discovery of sodium (Na^+) channel expression in human prostate cancer (PCa) cells led us to investigate the potential use of neuronal Na^+ channel blockers as inhibitors of PCa cells. Our initial studies discovered two classes of Na^+ channel blockers that were effective inhibitors of PCa cell proliferation. Both hydroxyamides (compounds 1 and 4) and a hydantoin (compound 5) were shown to inhibit the androgen-independent PCa cell line PC-3 *in vitro*. Electrophysiology showed that all compounds functionally block brain type II voltage-gated Na^+ channels (Nav1.2) expressed in *Xenopus laevis* oocytes. Long-term growth assays in androgen-independent PC-3 cells showed remarkable inhibition of cell growth, with cells growing to a maximum of 30% of controls with analogue 1. Further, our analogues demonstrated only marginal impact on cell viability over the same treatment interval. (Mol Cancer Ther. 2003;2:1149–1154)

Introduction

Prostate cancer (PCa) is the most common cause of cancer in men and the second leading cause of cancer death among men in the United States. Approximately 220,900 men will be diagnosed with PCa and ~28,900 will die from this disease in 2003 (1). For PCa, tumor initiation and progression often begins in men in the fourth and fifth decades of life and extends across many decades, resulting in invasive carcinoma (2). Because of the protracted course of this disease, the use of chemopreventive strategies or cytostatic strategies may be ideal in the treatment of PCa.

Received 1/8/03; revised 8/19/03; accepted 8/28/03.

The costs of publication of this article were defrayed in part by the payment of page charges. This article must therefore be hereby marked advertisement in accordance with 18 U.S.C. Section 1734 solely to indicate this fact.

Grant support: Jeffress Trust (M. L. B.), Paul Mellon Fund (M. L. B.), and University of Virginia Burger Center for Biological Sciences (M. L. B.). Additional funding from University of Delaware Research Foundation (R. A. S.) and Department of Biological Sciences, University of Delaware (R. A. S.).

Requests for Reprints: Milton L. Brown, Department of Chemistry, University of Virginia, McCormick Road, P. O. Box 400319, Charlottesville, VA 22904. Phone: (434) 982-3091; Fax: (434) 924-0798. E-mail: mlb2v@virginia.edu

Changes in cellular morphology are characteristic hallmarks of many pathological conditions. The capacity of a cell to alter its morphology and migrate is inherent to cancer cell metastasis. Although the precise biological mechanisms shaping cellular morphology during metastasis have not been elucidated, it is known that such changes involve cell-matrix interactions and cytoskeletal elements. The involvement of Na^+ channels in shaping cellular morphology has been described for neurons (3–5). The intracellular mechanisms through which Na^+ channel activity regulates prostate cellular morphology are still unclear, although ion channels have been implicated in several types of cellular behavior that could be related to the different stages of metastasis. These include proliferation (6), migration (7), and adhesion/interaction with the cellular matrix (8).

Voltage-gated ion channels, classically associated with impulse conduction in excitable tissues (9), are also found in a variety of epithelial cell types where their function is not well known. Nine mammalian Na^+ channel genes have been identified and found to be expressed and functional. These genes are >50% identical in amino acid sequence in the transmembrane and extracellular domains (10).

Several types of voltage-gated ion channels have been discovered in rat and human PCa cells (11). Several independent studies have also linked a prostate voltage-gated Na^+ channel α-subunit with the invasiveness of human prostate cell lines (LNCaP and PC-3; 12, 13) by Western blotting and flow cytometry. Electrophysiological studies using a whole-cell patch clamp indicated that the prostate cell Na^+ channel is sensitive to tetrodotoxin (TTX) at 1 μM, identifying the channel as voltage-dependent, TTX-sensitive Na^+ channel protein (14). Further, TTX has been shown to directly reduce the invasiveness of the cells *in vitro* (15), thus implicating the Na^+ channel as a viable target for anti-PCa research. Comparisons between rodent and human PCa cell lines led to the conclusion that the level of Na^+ channel expression is associated positively with the invasiveness of PCa cells *in vitro*. Encouragingly, both protein and functional studies strongly support Na^+ channel blockade as a viable mechanism for PCa cell inhibition.

Recently, the effect of four classical anticonvulsants on the secretion of prostate-specific antigen by LNCaP cells and interleukin-6 by DU-145 and PC-3 cells was measured by ELISA (16). The results demonstrated that both phenytoin and carbamazepine (Fig. 1), which inactivate voltage-gated Na^+ channels, inhibit the secretion of prostate-specific antigen by LNCaP and interleukin-6 by DU-145 and PC-3 cell lines (16). Additionally, the authors demonstrate a reduced capacity to form colonies in Matrigel on treatment with phenytoin. These data indicate further that Na^+ channel blockade is a strong candidate for effective treatment of PCa.

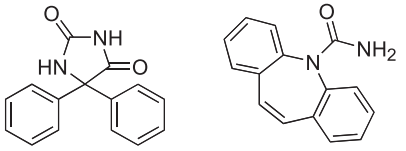

Figure 1. Chemical structures of phenytoin and carbamazapine.

Much of the information that we have learned about the phenytoin binding site in the neuronal voltage-gated Na^+ channel (NVSC) has been facilitated through the use of batrachotoxin (BTX). [^{3}H]-BTX experiments have revealed an allosteric relationship between BTX and the phenytoin binding site in brain tissue. This relationship enabled us to investigate the neuronal hydantoin receptor in the brain for conformation (17) and lipophilic (18) properties. Because there were little structural data about the phenytoin binding site on the NVSC, we embarked on the design, synthesis, and evaluation of a very defined series of compounds. The results of this work led to the development and publication (19) of the first predictive NVSC pharmacophore model. This model enabled the design and prediction of a new class of Na^+ channel blockers—the α-hydroxy-α-phenylamides. This study provides proof of principle that novel α-hydroxy-α-phenylamides are more potent inhibitors of the NVSC than the classic blocker phenytoin. Further, we provide evidence of their efficacy in the inhibition growth of the androgen-independent PCa cell line PC-3.

Materials and Methods

Chemistry

A summary of the scheme for chemical synthesis is provided in Fig. 2. All reactions requiring anhydrous conditions were performed in flame-dried glassware under Ar or N_2 atmosphere. Chemicals and solvents were either puriss. p.a. or purified by standard techniques. Melting points (mp) were determined with an Electrothermal MEL-TEMP mp apparatus and are uncorrected. ^{1}H and ^{13}C nuclear magnetic resonance (NMR) were performed on a GE 300-MHz spectrometer with Mac NMR 5.3 software. The chemical shifts are given in δ relative to tetramethylsilane (δ = 0 ppm) and the coupling constants J are given in Hz. The spectra were recorded in $CDCl_3$ as solvent at room temperature unless stated otherwise. High-resolution mass spectra (HRMS) were determined at the School of Chemical Science, University of Illinois Urbana-Champaign. Flash column chromatography was performed on silica gel (Merck grade 9385, 230–400 mesh, 60 Å), with eluent given in parentheses.

Preparation of Cyanohydrins from Ketones

To a flame-dried, three-neck, round-bottomed flask containing a magnetic stir bar and fitted with an inlet for maintaining an inert N_2 atmosphere, the ketone (1.0 eq) dissolved in dry CH_2Cl_2 was added. Trimethylsilyl cyanide (2.2 eq), potassium cyanide (KCN), and 18-crown-6 (10 mg each for every 1.0 mmol of ketone) were added, and the reaction was monitored by loss of the carbonyl peak (2250 cm^{-1}) in the infrared (IR). The CH_2Cl_2 was evaporated under reduced pressure, and a minimal amount of dry tetrahydrofuran (THF) was added. The mixture was cooled to 0°C, and 15% HCl (5 ml) was added and then stirred at room temperature for 2 h. The solution was combined with H_2O and extracted with Et_2O (3 × 25 ml), dried over $MgSO_4$, filtered, and concentrated to yield a thick dark oil. Because of stability concerns, the crude cyanohydrin was used without purification.

2-(3-Chloro-phenyl)-2-hydroxy-nonanenitrile was obtained as a dark oil (0.843 g, 76%). IR (m/z): 3430 (OH), 2240 (CN) cm^{-1}.

2-(4-Chloro-phenyl)-2-hydroxy-nonanenitrile was obtained as a yellow oil (0.4 g, 40%). IR (m/z): 3419 (OH), 2243 (CN) cm^{-1}.

2-Hydroxy-2-(4-methoxy-phenyl)-nonanenitrile was obtained as a dark oil (1.58 g, 100%). IR (m/z): 3400 (OH), 2220 (CN) cm^{-1}.

Preparation of α-Hydroxyamides from Cyanohydrins

The cyanohydrin was dissolved in 1,4-dioxane (2 ml) and added to a round-bottomed flask while stirring. The mixture was cooled to 0°C, and previously cooled (0°C)

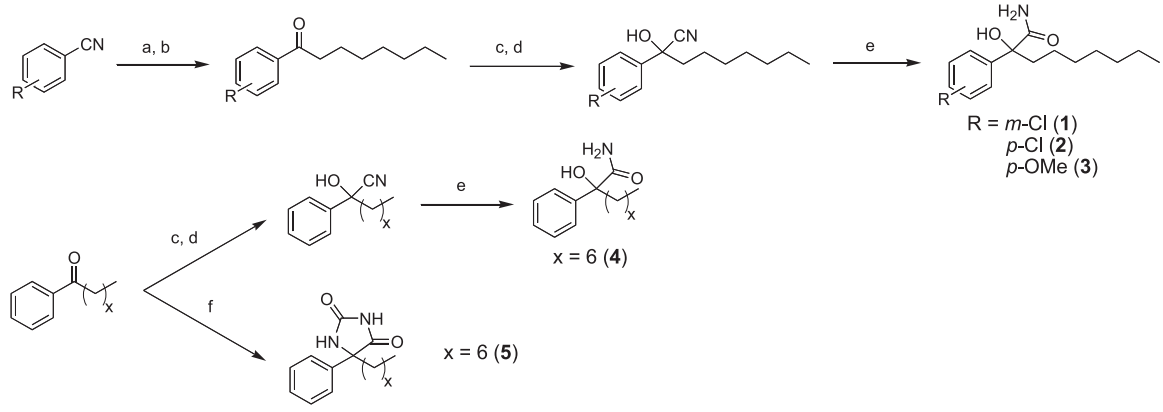

Figure 2. Reagents: (**a**) 1-bromoheptane, Mg, I_2, THF; (**b**) 15% HCl; (**c**) trimethylsilyl cyanide, KCN, 18-crown-6, CH_2Cl_2; (**d**) 15% HCl, THF; (**e**) 1,4-dioxane, concentrated HCl/HCl gas; (**f**) $(NH_4)_2CO_3$, KCN, 50% ethanol, 60°C.

concentrated HCl (0.2 ml for every 1 mmol of cyanohydrin) was added. HCl gas was then passed through the reaction mixture for 45 min at 0°C. The mixture was allowed to stir at room temperature overnight. The mixture was extracted with EtOAc (3 × 25 ml), dried over $MgSO_4$, filtered and concentrated to yield the crude α-hydroxyamide. Purification was performed by flash column chromatography (1:1 hexane:EtOAc), collecting all fractions with a component of $R_f = 0.28$ to yield the pure α-hydroxyamide.

2-(3-Chloro-phenyl)-2-hydroxy-nonanoic acid amide (**1**) was obtained as an off-white solid (1.86 g, 61%). mp = 78–79°C; ^{1}H NMR: δ 0.87 (t, 3H), 1.27 (m, 10H), 1.98 (m, 1H), 2.19 (m, 1H), 3.23 (broad, 1H), 5.96 (s, 1H), 6.55 (s, 1H), 7.24–7.59 (m, 4H); ^{13}C NMR: δ 14.57, 23.11, 23.82, 29.61, 30.10, 32.24, 39.91, 79.06,124.23, 126.27, 128.40, 130.15. HRMS (FAB) 284.1417 $(M + H)^+$.

2-(4-Chloro-phenyl)-2-hydroxy-nonanoic acid amide (**2**) was obtained as a white solid (0.37 g, 88%). mp = 95–97°C; ^{1}H NMR: δ 0.86 (t, 3H), 1.25–1.30 (m, 10H), 1.99 (m, 1H), 2.18 (m, 1H), 3.14 (broad, 1H), 5.64 (s, 1H), 6.46 (s, 1H), 7.30–7.54 (m, 4H); ^{13}C NMR: δ 14.56, 23.11, 23.85, 29.64, 30.13, 32.26, 39.95, 79.09, 109.86, 127.44, 128.99, 134.22, 141.34, 176.97. HRMS (FAB) 284.14 $(M + H)^+$.

2-Hydroxy-2-(4-methoxy-phenyl)-nonanoic acid amide (**3**) was obtained as a yellow solid (0.2 g, 17%). mp = 97–101°C; ^{1}H NMR: δ 0.83 (t, 3H), 1.12–1.50 (m, 10H), 2.36 (m, 2H), 3.78 (s, 3H), 5.62 (broad, 1H), 5.92 (t, 1H), 6.38 (broad, 1H), 6.83 (d, 2H), 7.30 (d, 2H); ^{13}C NMR: δ 14.59, 23.10, 29.55, 30.15, 30.39, 32.21, 55.81, 114.48, 128.39, 130.63, 134.25, 136.98, 159.77, 172.15. HRMS (FAB) 261.1732 $(M - H_2O)^+$.

2-Hydroxy-2-phenyl-nonanoic acid amide (**4**) was obtained as a white solid (2.8 g, 56%). mp = 98–99°C (lit. 91–92°C; 16); ^{1}H NMR: δ 0.86 (t, 3H), 1.07–1.47 (m, 10H), 2.01 (m, 1H), 2.2 (m, 1H), 3.52 (broad, 1H), 5.88 (s, 1H), 6.46 (s, 1H), 7.2–7.66 (m, 5H); ^{13}C NMR: δ 14.58, 23.13, 23.89, 29.67, 30.23, 32.30, 39.75, 79.09, 107.96, 125.95, 128.26, 128.94, 142.92. HRMS (FAB) 250.1807 $(M + H)^+$.

Preparation of Hydantoins from Ketones

Ketone (1 eq), KCN (2 eq), and $(NH_4)_2CO_3$ (4 eq) were added to a stirring solution of 50% ethanol (25 ml). The solution was warmed to 50–65°C for 12 h. The precipitate was filtered, and the filtrate was acidified to pH 2 using concentrated HCl. The resulting solid was filtered, and the filtrate was made basic using 3% potassium hydroxide. This was concentrated to one-half volume and filtered again. The combined solids were recrystallized from hot ethanol to give pure hydantoins.

5-Heptyl-5-phenyl-imidazolidine-2,4-dione (**5**) was obtained as a white solid (2.6 g, 65%). mp = 136–137°C (lit. 124–126°C; 16); ^{1}H NMR: δ 0.85 (t, 3H), 1.10–1.40 (m, 10H), 2.07 (m, 1H), 2.19 (m, 1H), 6.3 (broad, 1H), 7.11–7.49 (m, 5H), 7.90 (broad, 1H); ^{13}C NMR: δ 14.59, 22.97, 24.10, 29.43, 29.79, 32.08, 39.39, 68.68, 125.99, 128.22, 128.88, 139.76, 157.84, 177.20. HRMS (FAB) 275.1760 $(M + H)^+$.

[^{3}H]-BTX Assay

Briefly, rat forebrain membranes (10 mg tissue/well) were incubated with [^{3}H]-BTX (30–60 Ci/mmol). Reactions are carried out in 50-mM HEPES (pH 7.4) containing 130-mM choline chloride at 37°C for 60 min. The reaction was terminated by rapid vacuum filtration of the reaction contents onto glass fiber filters. Radioactivity trapped onto the filters was determined and compared with control values to ascertain any interactions of the test compound with the Na^+ channel site 2 binding site. Aconitine (1 μM) was used as a positive control (Sigma Aldrich, Inc., St. Louis, MO).

Na^+ Channel Electrophysiology

Rat Nav1.2 subunit cDNA engineered into pLCT1 was a generous gift from Dr. Alan L. Goldin (University of California-Irvine). Capped cRNA was transcribed *in vitro* from *Not*I linearized DNA template using T7 MessageMachine (Ambion, Inc., Austin, TX).

Xenopus laevis were anesthetized by immersion in 0.1% (w/v) 3-aminobenzoic acid (Sigma) and ovarian lobes were removed. Oocytes were dissociated enzymatically using 0.1% (w/v) collagenase (Sigma) in Ca^{2+}-free OR-2 solution (82.5-mM NaCl, 2.5-mM KCl, 1-mM $MgCl_2$, 5-mM HEPES [pH 7.6]). Prepared oocytes were microinjected with 23 or 46 nl of cRNA dissolved in water. Oocytes were incubated at 18°C in modified Barth's solution (88-mM NaCl, 1-mM KCl, 2.4-mM $NaHCO_3$, 0.3-mM $CaNO_3$, 0.41-mM $CaCl_2$, 0.82-mM $MgSO_4$, 15-mM HEPES, 100-μg/ml gentamycin sulfate [pH 7.6]).

Two-electrode voltage clamp recordings were performed 2–4 days after microinjection of cRNA using a Warner oocyte clamp (OC725C) interfaced to a Digidata 1322 A/D converter with Clampex software (v8; Axon Instruments, Union City, CA). Oocytes were continually perfused with Tyrodes solution (150-mM NaCl, 5-mM KCl, 1-mM $MgCl_2$, 2-mM $CaCl_2$, 10-mM glucose, 10-mM HEPES). Microelectrodes filled with 3-M KCl had resistances between 0.5–1 M ohms. Currents were elicited by a step depolarization from a holding potential of −100 to 0 mV for 90 ms at 15-s intervals. Currents were digitized at 33 kHz. All compounds were prepared as 100-mM stock concentrations in DMSO and diluted in Tyrodes solution. Data analysis was performed using Clampfit software (v8; Axon Instruments) and Origin (v6; Microcal Software, Northampton, MA). Statistical analyses were performed using a *t* test for normally distributed data as determined by the Kolmogorov-Smirnov test or the Rank Sum test for nonnormalized data (Sigmastat, SPSS, Inc., Chicago, IL). Averaged data are presented as means ± SEM.

Cells and Culture

All cell lines were cultured in T-medium (Life Technologies, Inc., Gaithersburg, MD; 20) + 5% FBS at 37°C under a 5% CO_2 environment unless indicated otherwise. The androgen-independent cell line PC-3 (21) was obtained from the American Type Culture Collection (Rockville, MD) and were carried in culture no more than 20 passages.

Crystal Violet Growth Assays

Cells were stained with crystal violet as an indirect measure of cell number as described previously (22, 23). Crystal violet assays were performed on days 1, 3, 5, and 7, with media and compound changes on days 0, 2, 4, and 6 of

Table 1. Effects of compounds on [^{3}H]-BTX binding

Compound (40 μM)	% [^{3}H]-BTX inhibition ± SEM
Phenytoin	30.4 ± 3.3 (n = 2)
1	46.1 ± 2.7 (n = 2)
2	48.4 ± 1.2 (n = 2)
3	52.6 ± 1.2 (n = 2)
4	55.7 ± 0.3 (n = 2)
5	58.1 ± 1.2 (n = 2)

All compounds tested at 40 μM.

culture. Each assay was run in triplicate for each drug or drug dose and repeated in this manner at least twice to provide a control for both intraassay and interassay variation. Cells were fixed to the bottom of each well with 1% glutaraldehyde in PBS for 15 min and then stained with 0.5% crystal violet in water for 15 min (Fisher Scientific, Newark, DE). The wells were gently flushed with water for 15 min and the plate was air dried before reading the absorbance on a Titertek Multiscan TCC/340 (Flow Laboratories, McLean, VA) microtiter plate reader at 560 nm. Cell amounts were determined as values relative to vehicle-treated controls.

Washout Experiments

Cells were grown as for crystal violet growth assays. On day 7, the media were replaced with fresh T-medium/5% FBS without drugs. One set continues to be cultured in phenytoin and one in control through day 13 with end points on days 9, 11, and 13. All values were normalized to day 7, vehicle treated. Crystal violet staining and measurement protocols are the same as for growth assays above.

Results and Discussion

We completed the synthesis of analogues shown in Fig. 2 and detailed in ''Materials and Methods.''

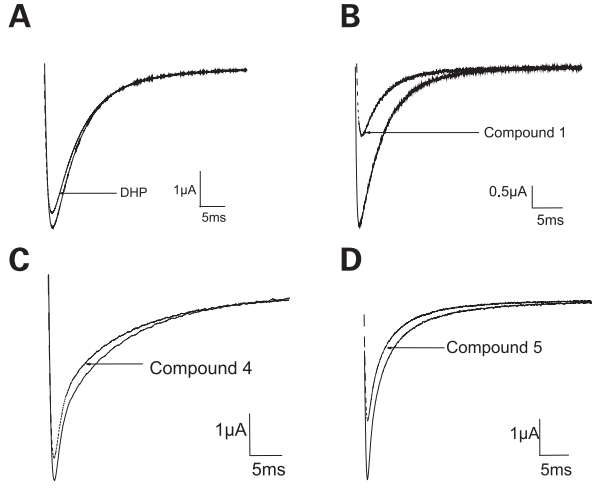

Figure 3. Effects of phenytoin (**A**) and novel compounds (**B**–**D**) on rNav1.2. Currents were elicited by a step depolarization from a holding potential of −100 to +10 mV for 50 ms at 15-s intervals. In each example, a control trace is superimposed with one recorded at maximum drug affect. All compounds were tested at 100-μM concentration.

Table 2. Effects of the various analogues on rNav1.2 expressed in *Xenopus* oocytes

Compound (100 μM)	% Block of rNav1.2 ± SEM
Phenytoin (DPH)	5.4 ± 1.7 (n = 6)
4	9.5 ± 0.9 (n = 8)
5	22.3 ± 4.3 (n = 7)
1	63.4 ± 5.2 (n = 6)

The synthetic methodology used was chosen due to its inherent ease of modification. We chose to initially synthesize phenyl ring modified hydroxyamides (*i.e.*, *m*, *p*-chloro, *p*-methoxy) because the unsubstituted phenylhydroxyamide (**4**) was previously shown to inhibit [^{3}H]-BTX binding (19). This standard medicinal chemistry approach allowed us to investigate the differences arising from the functional group substitutions on the phenyl ring.

The synthesis of α-hydroxyamides from nitriles or ketones was fairly straightforward. It is important to note the instability of the cyanohydrins obtained from trimethylsilyl cyanide addition to the ketone. After cleavage of the tetramethylsilane group from the alcohol, these compounds must be treated gently (*i.e.*, no heating); otherwise, they collapse to reform the initial ketone.

We initially evaluated these compounds for their ability to displace [^{3}H]-BTX binding to rat brain synaptoneurosomes. [^{3}H]-BTX is an important molecule in quickly assaying whether a compound has potential to bind to the neurotoxin binding site 2 on the Na^+ channel protein. Table 1 shows the percent inhibition of [^{3}H]-BTX binding when 40 μM of each compound were applied. We found that compounds **1**–**5** demonstrate very similar [^{3}H]-BTX activity (46–58% inhibition at 40 μM).

The results of this study indicate that all of these analogues bind to Na^+ channels more effectively than the anticonvulsant phenytoin.

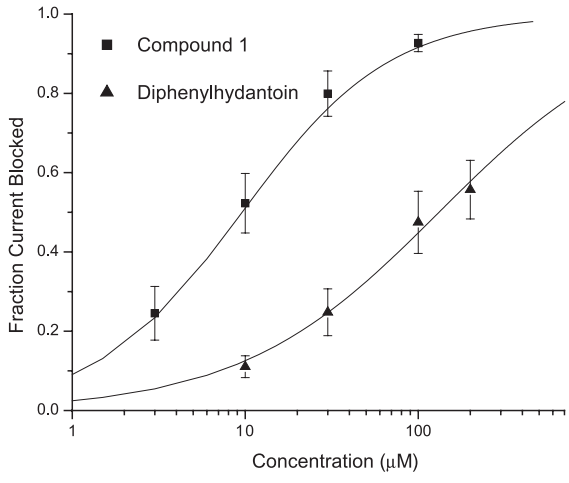

Figure 4. Dose-response curve for phenytoin and compound **1** on rNav1.2 expressed in *Xenopus* oocytes.

Table 3. Summary of dose-response data for compound 1 and phenytoin on rNav1.2 in *Xenopus* oocytes

Compound	IC_{50} (μM)	Slope
Phenytoin	173.8 ± 54.5	0.8 ± 0.1
1	10.4 ± 3.0	1.3 ± 0.1

Table 4. IC_{50} data most potent analogues on PC-3 cell proliferation in vitro

Compound	IC_{50} ± SEM (μM)
1	66.0 ± 0.7
2	66.8 ± 1.2
4	>100
5	66.0 ± 0.1

[^{3}H]-BTX is not a functional assay (ability to inhibit Na^+ flux into the cell) in that it is only useful for determining a compound's ability to bind to sites directly or allosterically associated with the [^{3}H]-BTX binding site. With this in mind, we evaluated compounds **1**, **4**, and **5** for *functional* ability to block Na^+ channel current by using the two-microelectrode voltage clamp technique on rNav1.2 expressed in *Xenopus* oocytes. These compounds were selectively chosen for this assay based on their inhibition of BTX binding (*i.e.*, the weakest binder and the two best binders). Fig. 3 shows the effects of these analogues (as well as phenytoin) on the rNav1.2 current, which were fully reversible with washout.

The results of this study, as summarized in Table 2, indicate that these analogues block Na^+ currents elicited by rNav1.2. Compound **1**, the most potent blocker, exhibited 63.4 ± 5.2% block of current at a concentration of 100 μM. It is clear from these data that binding to the Na^+ channel ([^{3}H]-BTX assay) does not fully describe a compound's effect on inhibiting Na^+ permeation through the cell. From [^{3}H]-BTX assays, compound **5** was clearly the best binder (**5** ≥ **4** > **3** > **2** > **1** > phenytoin); however, compound **1** demonstrated better functional inhibition of the channel (**1** > **5** > **4** > phenytoin).

We next evaluated the dose response of compound **1** for current block in rNav1.2 expressed in *Xenopus* oocytes. These data are shown in Fig. 4 and summarized in Table 3.

The data reveal that compound **1** is over 17 times better at inhibiting current than the standard Na^+ channel blocker phenytoin. These results clearly demonstrate that these compounds not only bind to Na^+ channels but also inhibit current in a concentration-dependent manner.

These data indicate that addition of an electron-withdrawing group to the phenyl ring leads to a more potent inhibitor of the Na^+ channel. Compound **1**, containing a *m*-chloro group, was about seven times more potent than the unsubstituted compound **4** in blocking Na^+ channels in *Xenopus* oocytes (Table 2). The hydantoin analogue, which is essentially diphenylhydantoin (DPH) with a long seven-carbon aliphatic chain instead of a phenyl ring substituent, proved to be more potent than DPH itself. These data indicate that a long hydrophobic chain is essential for optimal inhibition. Taken together, we have established that α-hydroxy-α-phenylamides functionally inhibit Nav1.2 Na^+ channels, a subtype known to be expressed in PC-3 cells.

Examination of the Na^+ channel blockers as potential inhibitors of the androgen-independent PCa cell line PC-3 revealed that these compounds were inhibitors of PC-3 cell growth in long-term growth assays (7 days with drug). The results of this growth assay for the PC-3 cell line are shown in Fig. 5.

The data demonstrate that all the hydroxyamide Na^+ channel blockers (**1–3**) inhibit PC-3 cell growth and that this effect is not transient. Hydroxyamide **4** also showed marginal effect on cell growth as did the Na^+ channel opener veratridine. Phenytoin was mildly stimulatory establishing a clear demarcation in effects between the hydroxyamide structural class and that of phenytoin. The resulting IC_{50} values for these active compounds are shown in Table 4. Despite the fact that phenytoin (DPH) was a poor inhibitor of PC-3 cell growth, hydantoin **5** exhibited an IC_{50} of 66 μM in inhibiting PC-3 cell growth, demonstrating that the seven-carbon chain is crucial for PC-3 cell growth inhibition. This result is further supported by [^{3}H]-BTX data that show progressive decreases in binding to Na^+ channels with shorter chain lengths (19). Altogether, we found that the trend in

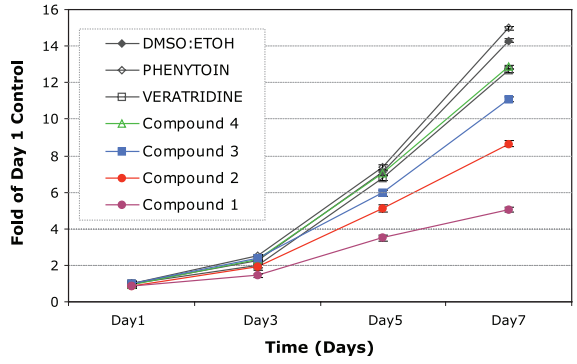

Figure 5. PC-3 cell proliferation assay. Crystal violet 7-day growth assay on PC-3 cells. All drugs were tested at a concentration of 40 μM.

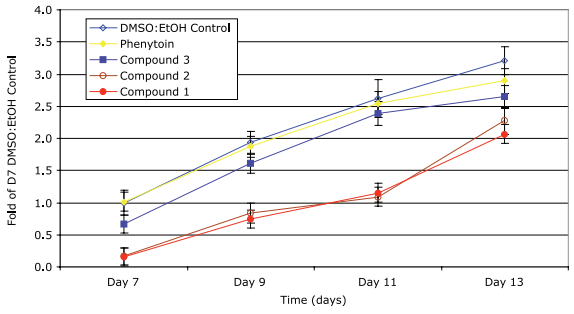

Figure 6. PC-3 washout fold of DMSO-D7 control. Drugs were washed out on day 7 and cell proliferation was monitored for 6 days.

potency seen in the cell proliferation assay (**5** ≈ **2** ≈ **1** > **4** > phenytoin) follows a similar trend to that seen in the functional ability (**1** > **5** > **4** > phenytoin) of these compounds to block Na^+ channels.

To determine the cytostatic nature of the inhibitory effect of the hydroxyamides, we performed 3-(4,5-dimethylthiazol-2-yl)-2,5-diphenyltetrazolium bromide (MTT) assays that could quantify the number of remaining viable cells after treatment with drug. This assay demonstrates that these compounds are predominately cytostatic inhibitors and have marginal impact on cell viability after 24 h of treatment. The largest reduction in cell viability is only seen at the highest dosage tested (100 μM) and the magnitude of this loss does not equal the more dramatic effect observed for the suppression of growth in the crystal violet assays. However, because the crystal violet assays are performed over 7 days, this assay did not answer questions about the long-term viability of the cells.

To ascertain whether the effects observed in the crystal violet growth assay were irreversible or reversible (*i.e.*, would the cells resume normal growth when compounds are removed), we performed washout experiments where after 7 days the drugs were removed from the growth media. These data are summarized in Fig. 6. As can be seen from this graph, the growth of PC-3 cells is fully restored when the inhibitory compounds are removed from the growth media, providing further evidence that these compounds are cytostatic inhibitors for the cells remaining on the dish.

Conclusion

Altogether, the results indicate a remarkable inhibition of androgen-independent prostate cancer growth by the hydroxyamide compound **1**. These data demonstrate that this compound quite effectively inhibited growth of PC-3 cells *in vitro*. The data indicate that with compound **1** the cells grow to a maximum of 30% of controls. The data imply that this is predominately a reversible, cytostatic effect; however, the nature of cell arrest and whether these effects are completely without cytotoxicity remain to be determined. In summary, this research has demonstrated that hydroxyamides actively inhibit PC-3 cell growth in a fully reversible, noncytotoxic manner and provide the basis of a targeted organic synthesis program to generate additional, perhaps more selective and potent, compounds for testing in the inhibition of PCa cell growth.

Acknowledgments

We thank Charles Bauer and Tammy Ransom (Novascreen Therapeutics, Hanover, MD) for [^{3}H]-BTX assays.

References

1. Jemal, A., Murray, T., Samuels, A., Ghafoor, A., Ward, E., and Thun, M. Cancer statistics, 2003. CA Cancer J. Clin., *53:* 5 – 26, 2003.

2. Colanzi, P., Santinelli, A., Mazzucchelli, R., Pomante, R., and Montironi, R. Adv. Clin. Pathol. Off. J. Adriat. Soc. Pathol., *3* (4)*:* 129 – 134, 1999.

3. Sretavan, D. W., Shatz, C. J., and Stryker, M. P. Modification of retinal ganglion cell axon morphology by prenatal infusion of tetrodotoxin. Nature, *336* (6198)*:* 468 – 171, 1988.

4. Mattei, C., Dechraoui, M. Y., Molgo, J., Meunier, F. A., Legrand, A. M., and Benoit, E. Neurotoxins targeting receptor site 5 of voltage-dependent sodium channels increase the nodal volume of myelinated axons. J. Neurosci. Res., *55* (6)*:* 666 – 173, 1999.

5. Matsutani, S. and Yamamoto, N. Neuronal regulation of astrocyte morphology *in vitro* is mediated by GABAergic signaling. Glia, *20* (1)*:* 1 – 9, 1997.

6. Niliius, B. and Wohlrab, W. Potassium channels and regulation of proliferation of human melanoma cells. J. Physiol., *445:* 243 – 252, 1992.

7. Komuro, H. and Rakic, P. Selective role of N-type calcium channels in neuronal migration. Science, *257:* 806 – 809, 1992.

8. Becchetti, A., Arcangeli, A., Bene, M. R., Olivotto, M., and Wanke, E. Response to fibronectin-integrin interaction in leukemia cells: delayed enhancing of a K^+ current. Proc. R. Soc. Lond. B, *248:* 235 – 240, 1992.

9. Anger, T., Madge, D. J., Mulla, M., and Riddall, D. Medicinal chemistry of neuronal voltage-gated sodium channel blockers. J. Med. Chem., *44* (2)*:* 115 – 137, 2001.

10. Goldin, A. L., Barchi, R. L., Caldwell, J. H., Hofmann, F., Howe, J. R., Hunter, J. C., Kallen, R. G., Mandel, G., Meisler, M. H., Nette, Y. B., Noda, M., Tamkun, M. M., Waxman, S. G., Wood, J. N., and Catterall, W. A. Nomenclature of voltage-gated sodium channels. Neuron, *28:* 365 – 368, 2000.

11. Laniado, M. E., Lalani, E. N., Fraser, S. P., Grimes, J. A., Bhangal, G., Djamgoz, M. B., and Abel, P. D. Expression and functional analysis of voltage-activated Na^+ channels in human prostate cancer cell lines and their contribution to invasion *in vitro*. Am. J. Pathol., *150* (4)*:* 1213 – 1221, 1997.

12. Diss, J. K. J., Archer, S. N., Hirano, J., Fraser, S. P., and Djamgoz, M. B. A. Expression profiles of voltage-gated Na^+ channel α-subunit genes in rat and human prostate cancer cell lines. Prostate, *48:* 165 – 178, 2001.

13. Smith, P., Rhodes, N. P., Shortland, A. P., Fraser, S. P., Djamgoz, M. B. A., Ke, Y., and Foster, C. S. Sodium channel protein expression enhances the invasiveness of rat and human prostate cancer cells. FEBS Lett., *423:* 19 – 24, 1998.

14. Grimes, J. A. and Djamgoz, M.B.A. Electrophysiological characterization of voltage-gated Na^+ current expressed in the highly metastatic Mat-LyLu cell line of rat prostate cancer. J. Cell. Phys., *175:* 50 – 58, 1998.

15. Grimes, J. A. and Djamgoz, M. B. A. Electrophysiological characterization of a TTX-sensitive Na^+ current in the highly metastatic Mat-LyLu rat prostate cancer cell line. J. Phys., *489:* 50P, 1995.

16. Abdul, M. and Hoosein, N. Inhibition by anticonvulsants of prostate-specific antigen and interleukin-6 secretion by human prostate cancer cells. Anticancer Res., *21* (3B)*:* 2045 – 2048, 2001.

17. Brouillette, W. J., Jestkov, V. P., Brown, M. L., Shamim Akhtar, M., Delorey, T. M., and Brown, G. B. Bicyclic hydantoins with bridgehead nitrogen. Comparison of anticonvulsant activities with binding to the neuronal voltage-dependent sodium channel. J. Med. Chem. *37:* 3289 – 3293, 1994.

18. Brown, M. L., Brown, G. B., and Brouillette, W. J. Effects of log P and phenyl ring conformation on the binding of 5-phenylhydantoins to the voltage-dependent sodium channel. J. Med. Chem., *40:* 602 – 607, 1997.

19. Brown, M. L., Van Dyke, C. C., Brown, G. B., and Brouillette, W. J. Comparative molecular field analysis of hydantoin binding to the neuronal voltage-dependent sodium channel. J. Med. Chem., *42:* 1537 – 1545, 1999.

20. Chang, S. M. and Chung, L. W. Interaction between prostatic fibroblast and epithelial cells in culture: role of androgen. Endocrinology, *125* (5)*:* 2719 – 2727, 1989.

21. Kaighn, M. E., Narayan, K. S., Ohnuki, Y., Lechner, J. F., and Jones, L. W. Establishment and characterization of a human prostatic carcinoma cell line (PC-3). Investig. Urol., *17* (1)*:* 16 – 23, 1979.

22. Gillies, R. J., Didier, N., and Denton, M. Determination of cell number in monolayer cultures. Anal. Biochem., *159* (1)*:* 109 – 113, 1986.

23. Thalmann, G. N., Sikes, R. A., Wu, T. T., Degeorges, A., Chang, S. M., Ozen, M., Pathak, S., and Chung, L. W. LNCaP progression model of human prostate cancer: androgen-independence and osseous metastasis. Prostate. *44* (2)*:* 91 – 103, 2000.